Strength enhancements in cold-formed structural sections – Part II: Predictive models

B. Rossi [(1)], S. Afshan [(2)] and L. Gardner [(3)]

[(1)] University of Liège, Liège, Belgium, [(2), (3)] Imperial College London, London, UK

Abstract

Cold-formed structural sections are manufactured at ambient temperature and hence undergo plastic deformations, which result in an increase in yield stress and a reduction in ductility. This paper begins with a comparative study of existing models to predict this strength increase. Modifications to the existing models are then made, and an improved model is presented and statistically verified. Tensile coupon data from existing testing programmess have been gathered to supplement those generated in the companion paper [1] and used to assess the predictive models. A series of structural section types, both cold-rolled and press-braked, and a range of structural materials, including various grades of stainless steel and carbon steel, have been considered. The proposed model is shown to offer improved mean predictions of measured strength enhancements over existing approaches, is simple to use in structural calculations and is applicable to any metallic structural sections. It is envisaged that the proposed model will be incorporated in future revisions of Eurocode 3 [2, 3].

1. Introduction

Cold-formed structural sections are widely used in construction, offering high strength and stiffness–to–weight ratios. Structural elements in a range of section shapes – tubular sections, including the familiar square, rectangular and circular hollow sections and the recently added elliptical hollow sections, and open sections such as angles, channels and lipped channels – are commonly used in building design. Cold-formed structural sections are manufactured at ambient temperature and hence undergo plastic deformations, which occur during both the sheet rolling and cross-section forming processes, causing strain hardening of the material. Upon application of stress, the strain hardened or cold-worked material follows a new loading path with an increased yield stress and ultimate stress, but reduced ductility. In metallic materials with a distinctly defined yield point, such as carbon steels, the stress-strain behaviour becomes rounded following the cold-forming process. Non-uniformity in the material properties around cold-formed sections also exist, due to the varying level of plastic

strain experienced, with the corner regions being the most influenced. Materials, such as stainless steel, with rounded stress-strain behaviour and significant strain hardening show a more pronounced response to cold-working.

With increasing emphasis being put on the sustainable use of resources, fully exploiting material properties in structural design is paramount. The performance of finite element (FE) models is also often highly sensitive to the prescribed material parameters, making an accurate representation of the material characteristics essential. Therefore, developing suitable predictive models for harnessing the increases in material strength caused by plastic deformations, experienced during the cold-forming production routes, is required.

In this paper, predictive models from the literature for determining the strength enhancements observed in cold-formed metallic sections are reviewed. Two recently proposed predictive models, developed by Cruise and Gardner [4] and Rossi [5], have been assessed extensively. Improvements to the existing models have been made and a new predictive model is presented. In the companion paper [1], a laboratory testing programme was conducted to measure the level of strength enhancement induced in cold-formed structural sections. Material tests on a total of 51 flat coupons and 28 corner coupons, extracted from the flat faces and corner regions of SHS and RHS tubes, were performed. The generated tensile coupon test results, combined with those from existing experimental programmes, have been used to validate the predictions from the models and make comparisons between the presented predictive equations. In total, the collated database covers a range of structural section types – square hollow sections (SHS), rectangular hollow sections (RHS), circular hollow sections (CHS), angles, lipped channels and hollow flange channel sections from both cold-rolling and press-braking fabrication processes – and structural materials, namely carbon steel and stainless steel (EN 1.4301, 1.4306, 1.4307, 1.4318, 1.4404, 1.4571, 1.4401, 1.4016, 1.4003, 1.4509, 1.4512, 1.4462 and 1.4162).

2. Production routes

Cold-rolling and press-braking are the two methods commonly employed in the manufacture of light gauge cold-formed structural sections. In press-braking the sheet material is formed into the required shape by creating individual bends along its length. It is a semi-automated process used to produce open sections, such as angles and channels, in limited quantities. Air press-braking, where elastic spring back is allowed by over-bending the material, is more

commonly adopted than coin press-braking, where the die and the tool fit into one another. Cold-rolling is an automated continuous bending process in which the gradual deformation of the uncoiled metal sheet through a series of successive rollers produces the final cross-section profile.

In case of tubular box sections, the flat metal sheet is first rolled into a circular tube and is welded closed. It is subsequently deformed into a square or rectangle by means of dies as depicted in Fig. 1. The tube's cross-section is initially circular whereas the cross-section at the end of the process is a square or rectangle with round corners.

3. Predictive models

3.1 Introduction

Finite element simulations of processes involving complex contact and springback problems, such as stamping processes, can be achieved with good accuracy. But, simulating the continuous cold-rolling process using FE methods requires complicated three-dimensional models which becomes computationally expensive due to the relatively high mesh density that must be employed to result in accurate solutions. As examined by Rossi et al. [6], many recent studies have focused on comparisons between different types of finite element formulations and integration schemes for modelling the plastic deformations occurring in the highly bent corner regions of the sections, the change in thickness or springback as well as accurate modelling of the material stress-strain response. But, FE modelling of this continuous process of fabrication is usually not used for determining the strength enhancement occurring in cold-formed sections. Alternatively, closed-form analytical solutions, such as that of Quach et al. [7], of the residual stress distribution and plastic strains induced during press braking exist for elastic-plastic plane strain pure bending with materials assumed to obey the von Mises yield criterion. The analytical models developed to date are restricted to coiling followed by uncoiling and press braking. In the current study, predictive models for the strength increases in the corner regions and flat faces of cold-formed cross-sections are examined.

3.2 Literature review

Early studies of the strength enhancement in the corner regions of cold-formed carbon steel sections were carried out by Karren [8]. A power model to predict the strength increases in the corner regions of cold-formed sections, in terms of the yield stress of the unformed sheet material and the internal corner radius to thickness ratio was proposed. The model was developed based on available test data, including specimens formed by both cold-rolling and press-braking processes. The author suggested that since the corner regions typically represent 5% to 30% of the total cross-sectional area, the influence of the enhanced corner strength should be incorporated in structural calculations. Coetzee et al. [9] performed an experimental study into strength enhancements in cold-formed stainless steel sections. Material tests on press-braked lipped channel sections of three stainless steel grades (EN 1.4301, 1.4401 and 1.4003) were conducted. Karren's expression was later modified by van den Berg and van der Merwe [10] on the basis of Coetzee et al.'s test data and further test data on stainless steel single press-braked corner specimens in grades EN 1.4301, 1.4016, 1.4512 and 1.4003. Gardner and Nethercot [11] studied test data from cold-rolled box sections and observed a linear relationship between the 0.2% proof strength of the corner regions and the ultimate strength of the flat faces.

Ashraf et al. [12] analysed all stainless steel test results, from a variety of fabrication processes, to investigate the application of the predictive equations proposed by van den Berg and van der Merwe [10]. Comparisons of the predicted strength and the test results showed that modifications to the models were required. Three empirical predictive models for the evaluation of the corner yield strength were proposed. Two power models based on the properties (0.2% proof strength and the ultimate tensile strength) of the unformed sheet material were developed to predict the corner 0.2% proof strength of both cold-rolled and press-braked sections. The linear expression proposed by Gardner and Nethercot [11], to predict the 0.2% proof strength of the corners in cold-rolled box sections was also recalibrated. Furthermore, in order to obtain full insight into the influence of cold-work on the corner material properties, an equation to predict the ultimate tensile strength of the corner material was developed.

Cruise and Gardner [4] later recalibrated the Ashraf et al. [12] expressions in light of further stainless steel experimental data and proposed two revised expressions to predict the enhanced corner strength of press-braked and cold-rolled sections. In addition, expressions

for evaluating the 0.2% proof stress and the ultimate tensile stress of the flat faces of cold-rolled box sections were developed. Similarly, based on corner material test results on structural carbon steel box sections, Gardner et al. [13] modified the predictive model given in the AISI Specification for the Design of Cold-formed Steel Structural Members [14]. Values of the coefficients in the predictive equation were proposed that enabled the model to be applied to the assessment of the enhanced corner strength of cold-rolled square and rectangular hollow sections.

An alternative formula to evaluate the enhanced 0.2% proof strength in the flat faces and corner regions of cold-formed sections, using the properties of the unformed sheet material and the final cross-section geometry, was proposed by Rossi [5]. The proposed equation is established using the inverted Ramberg-Osgood material model without introducing empirical parameters, allowing its application to a range of non-linear metallic materials.

3.3 Cruise and Gardner [4] predictive model

Cruise and Gardner [4] carried out an extensive experimental study of cold-formed stainless steel structural sections made of grade EN 1.4301 material, produced from both cold-rolling and press-braking production routes. Based on the experimental results, including tensile coupon tests and hardness tests, the distributions of the 0.2% proof strength and ultimate tensile strength around a series of cold-rolled box sections and press-braked angle sections were identified. The generated test data were combined with all other available published experimental data and used to develop models for predicting the strength enhancements around stainless steel sections due to cold-forming. The experimental observations showed that, for press-braked sections, the enhancements are confined to the corner regions, whereas cold-rolled box sections also exhibited significant strength increases in the flat faces, indicating that the flat faces in cold-rolled box sections also experience plastic deformations during forming. New models were therefore proposed to predict the strength enhancements in the flat faces of cold-rolled box sections. Expressions for the 0.2% proof stress $\sigma_{0.2,f,pred}$ and the ultimate tensile stress $\sigma_{u,f,pred}$, Eqs. (1) and (2) respectively, were provided, in which t, b and h are the section thickness, width and depth respectively, and $\sigma_{0.2,mill}$ and $\sigma_{u,mill}$ are the 0.2% proof stress and ultimate tensile stress of the unformed material, as provided by the mill certificate. The two key driving parameters in the models were the strain experienced during section forming and the potential for strength enhancement of the material [4].

$$\sigma_{0.2,f,pred} = \frac{0.85\sigma_{0.2,mill}}{-0.19 + \dfrac{1}{12.42\dfrac{\pi t}{2(b+h)} + 0.83}} \quad (1)$$

$$\sigma_{u,f,pred} = \sigma_{u,mill}\left(0.19\left(\frac{\sigma_{0.2,f,pred}}{\sigma_{0.2,mill}}\right) + 0.85\right) \quad (2)$$

Existing literature models were also modified to predict the strength enhancement in the corner regions of cold-rolled and press-braked stainless steel sections. The simple power model proposed by Ashraf et al. [12] was recalibrated based on a more comprehensive experimental database to predict the 0.2% proof stress of the corners in press-braked sections. For cold-rolled sections, the model presented in Gardner and Nethercot [11] and later recalibrated by Ashraf et al. [12], providing a linear relationship between the 0.2% proof stress of the formed corners and the ultimate strength of the flat faces, was again updated. The proposed expressions for the corner strength enhancement $\sigma_{0.2,c,pred}$ are given by Eqs. (3) and (4) for press-braked sections and cold-rolled sections, respectively, in which r_i is the internal corner radius. The experimental data also indicated that, the corner strength enhancement extends beyond the curved corner region for cold-rolled sections, and it is confined to the corner region for press-braked sections. It was therefore proposed that Eq. (4), for cold-rolled sections, should be used to predict a uniform strength enhancement for the corner region plus an extension of 2t, where t is the material thickness, beyond the corner radius into the flat faces of the section.

For press-braked section:

$$\sigma_{0.2,c,pred} = \frac{1.673\sigma_{0.2,mill}}{\left(r_i/t\right)^{0.126}} \quad (3)$$

For cold-rolled section:

$$\sigma_{0.2,c,pred} = 0.83\,\sigma_{u,f,pred} \quad (4)$$

3.4 Rossi [5] predictive model

Rossi [5] examined the through-thickness residual stress distributions and strength enhancements induced during cold-forming of sections composed of non-linear metallic materials. The proposed model for predicting the cold-work strength enhancement is essentially based on the determination of the plastic strains caused during the fabrication process and evaluation of the corresponding stresses, through an appropriate material model. The cold-rolling fabrication process was broken down into four key steps: (A) coiling of the sheet material, (B) uncoiling of the sheet material, (C) forming into a circular section and (D) subsequent deforming into a square or rectangular section. The flat faces of cold-rolled hollow sections were thus assumed to undergo coiling and uncoiling in the rolling direction followed by bending and unbending, in the direction perpendicular to the rolling direction. Analysis of the results showed that the plastic strain from both the sheet forming and cross-section forming processes contribute to the overall strength enhancement of the flat faces of cold-rolled box sections. However, Step C, forming into a circular section, was found to have the greatest influence on strength enhancement in the flat faces of cold-rolled box sections and was used as the dominant stage for subsequent analysis. For the corner regions, in both cold-rolled and press-braked sections, the final formation of the corner was considered as the dominant stage of the process.

The induced plastic strains associated with the dominant stages of the flat face and corner forming processes were determined. Assuming pure bending, the maximum transverse strain experienced by the section face during the formation of the circular tube (step C) was taken as $\varepsilon_f = \pi t/2(b+h)$. Similarly, the maximum strain induced during corner forming was taken as $\varepsilon_c = (t/2)/r_i$. The symbols are defined in Fig. 2. Note that these are essentially the same strains considered by Cruise and Gardner [4].

The inverted compound Ramberg-Osgood material model, proposed by Abdella [15] was employed within the predictive model to mimic the stress-strain response of the unformed sheet material, with key points obtained from the mill certificate. The maximum surface plastic strains were incorporated into the material model to deduce the ensuing enhanced strength. The resulting predictive model [5] is given by Eq. (5). The proposed formula may be used to evaluate the strength enhancement $\sigma_{0.2,f \text{ or } c,\ pred}$ in the flat faces of cold-rolled box sections and the corner regions of both cold-rolled sections and press-braked sections, based on the appropriate radius: $R = (b+h)/\pi$ for flat faces and $R = r_i$ for the corner regions.

$$\frac{\sigma_{u,mill}}{\sigma_{0.2,f\ or\ c,pred} - \sigma_{0.2,mill}} = C_1\left(\frac{R}{t/2}\right) + C_2\left(\frac{R}{t/2}\right)^{\alpha} \quad (5)$$

in which,

$$C_1 = \frac{\varepsilon_{t,0.2}}{r_2}\frac{\sigma_{u,mill}}{\sigma_{0.2,mill}} \quad (6)$$

$$C_2 = \frac{\left(r^* - 1\right)\varepsilon_{t,0.2}}{r_2\left(\varepsilon_u - \varepsilon_{t,0.2}\right)^{p^*}}\frac{\sigma_{u,mill}}{\sigma_{0.2,mill}} \quad (7)$$

where, $r_2 = E_{0.2}\varepsilon_{t,0.2}/\sigma_{0.2}$, $E_{0.2} = \sigma_{0.2}E/(\sigma_{0.2} + 0.002nE)$, $r^* = E_{0.2}(\varepsilon_u - \varepsilon_{t,0.2})/(\sigma_u - \sigma_{0.2})$, $p^* = r^*(1 - r_u)/(r^* - 1)$, $r_u = E_u(\varepsilon_u - \varepsilon_{t,0.2})/(\sigma_u - \sigma_{0.2})$, $E_u = E_{0.2}/[1+(r^* - 1)m]$, $m = 1+3.5\sigma_{0.2}/\sigma_u$, $\alpha = 1 - p^*$ and $\varepsilon_{t,0.2} = 0.002+ \sigma_{0.2}/E$.

4. Comparisons of existing predictive models

4.1 Experimental database

In order to assess the wider applicability of the predictive models presented in Sections 3.3 and 3.4, tensile coupon data from a broad spectrum of existing testing programs have been gathered [9, 10, 13, 16-28] to supplement those obtained in the companion paper [1]. The collated database covers a range of structural section types – CHS, SHS, RHS, angles, lipped channel sections (LCS) and hollow flange channel sections (HFCS) from both cold-rolling and press-braking fabrication processes, as illustrated in Fig. 3, and a range of structural materials including carbon steel grades and austenitic (EN 1.4301, 1.4306, 1.4307, 1.4318, 1.4404, 1.4571,1.4401), ferritic (EN 1.4016, 1.4003, 1.4512, 1.4509), duplex (EN 1. 4462) and lean duplex (EN 1.4162) stainless steel grades. In order to investigate the strength enhancement due to face forming processes in cold-rolled sections, reported tensile coupon tests for this portion of the section have been used. Table 1 provides a summary of the collected database for the flat faces of the cold-rolled sections analysed herein. Based on the available published corner test data, for both cold-rolled and press-braked sections, the performance of the predictive models for corners has also been assessed. The compiled database for corner coupon tests considered in this study is summarised in Table 2.

The collected information includes the section geometric dimensions, mill certificate material properties – $\sigma_{0.2,mill}$ and $\sigma_{u,mill}$ – and the measured material properties of the formed sections – the 0.2% proof stress $\sigma_{0.2,test}$ and the ultimate tensile stress $\sigma_{u,test}$. For cold-formed sections, the mill test is carried out on sheet material prior to section forming in the transverse direction, perpendicular to the rolling direction, and the results are supplied by the manufacturer. The Ramberg-Osgood material model parameters, required for the Rossi [5] model, were sourced from [1, 29, 30] and the relevant material properties were obtained from EN 1993-1-1 [3] for carbon steel sections and EN 10088-1 [31] for stainless steel sections.

4.2 Comparison of predictive models

This section provides a broad comparison, in terms of both the accuracy of the predictions and the ease of use, of the two predictive models. Numerical comparisons, including the mean and coefficient of variation (COV), of the two predictive models with the test data, in terms of the predicted strength to the test strength ratio, are presented in Tables 3 and 4 for flat faces and corner regions, respectively. Although the proposed predictive model for flat faces of cold-rolled sections provided by Cruise and Gardner [4] was calibrated only for stainless steel, it has also been applied herein to carbon steel test data for comparison purposes and the results are shown in Table 3 in brackets.

Analysis of the results shows that for the flat faces of cold-rolled stainless steel sections, the predictive model from Rossi [5] is able to predict more accurate results, in terms of the mean value, than the predictive equation proposed by Cruise and Gardner [4] but, has higher scatter. The results for the corner regions show that for stainless steel, the Cruise and Gardner [4] model offers more accurate prediction of the test data with lower scatter. Also, Rossi [5] and the modified AISI [13] predictions for the corner strength enhancements of carbon steel sections are in good agreement, with the former showing a lower scatter of 0.09.

As far as the flat faces of cold-rolled sections are concerned, both models use the same measure of cold-work induced plastic strain in their formulations, but different material models. The Rossi [5] model employs the compound Ramberg-Osgood material model whereas, Cruise and Gardner [4] assume linear hardening material behaviour for stainless steel with the material model incorporated into the predictive model coefficients resulting in the same relative enhancement whatever the material. As a result, while the Rossi [5] predictive model may be applied to any non-linear material, the Cruise and Gardner [4]

model is specific to structural sections with the material for which the models were calibrated against, which included austenitic stainless steel grade EN 1.4301. Moreover, strength enhancements should be predicted once any finite plastic strains are experienced and Cruise and Gardner [4] formulation is not in accordance with this principle. Owing to the complicated mathematical form and the number of input parameters required to evaluate the cold-work induced strength enhancement from Rossi's [5] predictive equation, it is lengthy to implement in design calculations. In order to overcome the shortcomings of the two predictive models, a new concise and accurate predictive model is proposed in the next section.

5. Extension of the predictive models

5.1 Introduction

In this section a simple and accurate method for predicting the strength enhancement in cold-formed structural sections is presented. The model development is based on the same concept as used in the Rossi [5] predictive model, which involves the determination of the cold-work induced plastic strain followed by the evaluation of the corresponding stress from the stress-strain response of the unformed sheet material, using an appropriate material model. Given the scatter in the test data, as shown in Figs. 4 and 5 for flat faces and corner regions, respectively, and the assumptions made in simplifying the forming processes, using a simple material model, in place of the compound Ramberg-Osgood model, is deemed more appropriate. In addition, analysis of the results shows that the plastic strain from both the sheet forming and cross-section forming processes contribute to the overall strength enhancement of the flat faces of cold-rolled box sections and should be allowed for in predicting the resulting strength enhancements.

5.2 Material stress-strain models

In order to represent the stress-strain response of the unformed sheet material, the suitability of a power law model and a tri-linear material model with strain hardening, Eqs. (8) and (9), respectively, have been assessed. The parameters which define each model are based on the key material properties of the unformed sheet, as provided in the mill certificate.

$$\sigma = p\varepsilon^{q} \qquad \text{for} \quad 0 \le \varepsilon \le \varepsilon_u \tag{8}$$

$$\begin{aligned} \sigma &= \sigma_{0.2} + \left(\frac{\sigma_u - \sigma_{0.2}}{0.5\varepsilon_u - \varepsilon_{0.2}} \right) \left(\varepsilon - \varepsilon_{0.2} \right) && \text{for} \quad \varepsilon_{0.2} < \varepsilon \le 0.5\varepsilon_u \\ \sigma &= \sigma_u && \text{for} \quad 0.5\varepsilon_u < \varepsilon \le \varepsilon_u \end{aligned} \tag{9}$$

The power law model parameters, p and q, are calibrated such that the function passes through the 0.2% proof stress and corresponding total strain ($\varepsilon_{t,0.2}$,$\sigma_{0.2}$) and the ultimate tensile stress and corresponding total strain (ε_u,σ_u) points. The model's inability to provide a good fit to the actual stress-strain response at low strains will not influence the predicted strength due to the relatively large magnitude of the plastic strains induced during cold-forming processes.

For the tri-linear model, the first stage has a slope E, taken as the material initial Young's modulus, up to the yield point, defined as the 0.2% proof stress and the corresponding elastic strain $\varepsilon_{0.2} = \sigma_{0.2}/E$. The strain hardening slope is determined as the slope of the line passing through the defined yield point ($\varepsilon_{0.2}$, $\sigma_{0.2}$) and a specified maximum point (ε_{max}, σ_{max}) with ε_{max} taken as $0.5\varepsilon_u$, where ε_u is the ultimate tensile strain, and σ_{max} is taken as the ultimate tensile stress σ_u. A similar approach has been recommended in EN 1999-1-1 [32] for modelling the stress-strain response of aluminium alloys. In order to prevent significant over-predictions of strength at large strains, a maximum stress limit equal to the ultimate tensile stress σ_u has been added. No strength enhancement would result from strains less than the yield strain; hence the initial part of the model will not be used for strength enhancement predictions. The strain at the ultimate tensile stress ε_u of the unformed sheet material, required in both material models, is not provided in the material mill certificate. Hence, the expression given in Annex C of EN 1993-1-4 [2] for modelling the stress-strain response of stainless steels, which was further verified in the companion paper [1], has been employed herein.

5.3 Cold-worked induced plastic strains

Cold-work plastic strains are induced during both the coiling and uncoiling of the sheet material and the cross-section forming processes. The plastic strain components from both the sheet forming and cross-section forming processes therefore contribute to the overall strength enhancement of the flat faces of cold-rolled box sections whereas for corners of cold-rolled sections and press-braked sections, the plastic strains from the formation of the

corner are generally much larger in magnitude than the plastic strains induced prior to corner forming.

The through thickness strain induced during the coiling/uncoiling processes is related to the internal coil radius and the radial location of the sheet in the coil. The critical coil radius associated with the initiation of through thickness plastic strains from sheet coiling depends on the thickness and material properties of the sheet. If the coil radius is greater than this critical radius, no plastic strains are introduced; otherwise, varying degrees of through thickness plastic strains are produced. As it is not possible to provide an exact measure of the plastic strains associated with the coiling/uncoiling processes, due to the unknown value of the coil radius coinciding with the as-formed member, this strain may be determined on the basis of an average coil radius $R_{coiling}$ = 450 mm, as recommended in Moen et al. [33].

The total plastic strain experienced by the flat faces of cold-rolled box-sections is taken as the sum of the strains from the coiling, uncoiling, formation of the circle and crushing into the final cross-section geometry – referred to as steps A, B, C and D in Rossi [5]. The amount of straining is dependent on the history of deformation, the location away from the middle surface of the sheet, the distance between the neutral surface and the middle surface, and the bending curvature. Also, the deformation history involves elastic unloading: in reality, step D should not be considered the same as step C, but incorporating rigorous strain calculations will complicate the model. Therefore, reverse bending (uncoiling and formation of the final cross-section) is assumed to cause the same magnitude of strain as bending. Hence, the strains from the sheet uncoiling and formation of the final geometry are taken as equal and opposite to the strains from coiling and formation of circular tube, respectively. In addition, the maximum surface plastic strains was used in the predictive models presented in Sections 3.3 and 3.4, but a more appropriate measure for predicting the strength enhancements is in fact the through thickness averaged plastic strain; and this has been employed herein. With the assumption of a linearly varying strain distribution through the material thickness and a bending neutral axis that coincides with the material's mid-thickness, the through thickness averaged plastic strain is given as half of the maximum surface strain. Hence, the through thickness averaged plastic strains for the flat faces $\varepsilon_{f,av}$ and corner regions $\varepsilon_{c,av}$ to be used in the new predictive model are:

$$\varepsilon_{f,av} = \left[(t/2)/R_{coiling}\right] + \left[(t/2)/R_f\right] \quad (10)$$

$$\varepsilon_{c,av} = 0.5\left[(t/2)/R_c\right] \quad (11)$$

where, $R_f = \frac{b+h-2t}{\pi}$ and $R_c = r_i + \frac{t}{2}$

5.4 Analysis of results and design recommendations

The experimental database presented in Section 4.1 has been used to investigate the applicability of the two simple stress-strain models with the through thickness averaged plastic strain measures introduced in Sections 5.2 and 5.3 for predicting the strength enhancement in cold-formed sections. Numerical comparisons, including the mean and coefficient of variation (COV), of the predictions from both material stress-strain models with the test data, in terms of the predicted strength to the test strength ratio, are presented in Tables 5 and 6 for the flat faces and corner regions, respectively.

Analysis of the results shows that for both the flat faces and corner regions, the power law material model gives more accurate results in terms of both the mean and the COV, than the linear hardening material model. The power law model and the Rossi [5] model give similar mean values of 1.01 and 0.97, respectively for the flat faces of cold-rolled stainless steel and carbon steel sections. As far as the corner regions of cold-formed sections are concerned, the Rossi [5] model over-predicts the test data, highlighting that the use of the maximum surface plastic strain is not appropriate, while the power law model with the through thickness averaged strain measure offers safer predictions. Overall, the proposed power law material model with the new through thickness averaged plastic strain predictions are in good agreement with the test data and may be employed to predict the strength enhancement in cold-formed structural sections.

The developed predictive model is used for determining the tensile 0.2% proof strength of cold-formed sections and is based on the tensile material properties of the unformed sheet material. Owing to the asymmetric stress-strain response of stainless steel in tension and compression [11, 24], its material properties are often supplied in both tension and compression in structural design standards. The AS/NZS 4673 [34] and SEI/ASCE-8 [35] standards provide both tensile and compressive material properties while the EN 1993-1-4 [2]

only considers tensile material properties. Existing data on tensile and compressive coupon tests from the literature [9, 11, 24-27, 36] were analysed, see Fig. 6, and it was shown that the compressive 0.2% proof strength is on average 5% lower than that for tension. This finding is to be allowed for in the predictive model.

Test data on stainless steel cold-formed tubular members in compression and bending were also gathered and statistical analyses in accordance with EN 1990- Annex D [37] were performed to assess the reliability of the current EN 1993-1-4 [2] design guidelines. To allow for the increased variability associated with the prediction of material strength, as opposed to adopting minimum specified values, a factor of 0.90 is proposed to be used in conjunction with the new predictive equation to maintain the same level of reliability as current codified guidelines. The predictive equation for determining the enhanced 0.2% proof stress of cold-formed structural sections, allowing for asymmetry in the stress-strain response and the required reliability level through the 0.85 factor (≈ 0.95×0.90), is presented in its final form in Eqs. (12) and (13) for the flat faces and corner regions, respectively.

$$\sigma_{0.2,f,pred} = 0.85\left[p\left(\varepsilon_{f,av} + \varepsilon_{t,0.2}\right)^{q}\right] \qquad \text{but} \le \sigma_{u,mill} \tag{12}$$

$$\sigma_{0.2,c,pred} = 0.85\left[p\left(\varepsilon_{c,av} + \varepsilon_{t,0.2}\right)^{q}\right] \qquad \text{but} \le \sigma_{u,mill} \tag{13}$$

The coefficient p and the exponent q may be calculated directly from the basic properties of the unformed material from the mill certificates, as given by Eqs. (14) and (15), respectively. In the absence of the mill certificate values, the minimum codified material properties may be used.

$$p = \frac{\sigma_{0.2,mill}}{\varepsilon_{t,0.2}^{\ q}} \tag{14}$$

$$q = \frac{\ln\left(\sigma_{0.2,mill}/\sigma_{u,mill}\right)}{\ln\left(\varepsilon_{t,0.2}/\varepsilon_{u}\right)} \tag{15}$$

Following the findings of Cruise and Gardner [4], for the press-braked sections, the enhanced corner strength is confined to the curved corner region only of area A_c and for cold-rolled box sections, it extends by 2t, where t is the material thickness, beyond the corner radius into the flat faces of the section. Hence, the cross-section weighted average enhanced 0.2% proof

stress for press-braked sections and cold-rolled box sections may be determined from Eqs. (16) and (17), respectively.

For press-braked sections:

$$\sigma_{0.2,section} = \frac{\left(\sigma_{0.2,c,pred} A_{c,pb}\right) + \left(\sigma_{0.2,mill}\left(A - A_{c,pb}\right)\right)}{A} \quad (16)$$

For cold-rolled sections:

$$\sigma_{0.2,section} = \frac{\left(\sigma_{0.2,c,pred} A_{c,rolled}\right) + \left(\sigma_{0.2,f,pred}\left(A - A_{c,rolled}\right)\right)}{A} \quad (17)$$

where, $A_{c,pb} = A_c = (n_c \pi t/4)(2r_i + t)$, $A_{c,rolled} = A_c + 4n_c t^2$, A= gross cross-sectional area of the section and n_c is the number of 90° corners in the section.

The new predictive model was evaluated against the test data presented in Section 4.1. The method offers, on average, 19% and 36% strength enhancements relative to the minimum codified strength values provided in EN 1993-1-4 [2] and EN 1993-1-1 [3], for the flat faces and corner regions, respectively. The new proposed predictive model is simple to use in structural calculations and is applicable to any metallic structural sections.

6. Conclusions

A review of predictive models from the literature for harnessing the strength increases in cold-formed sections as a result of plastic deformation during production has been carried out. Two recently proposed predictive models, developed by Cruise and Gardner [4] and Rossi [5], were assessed extensively. Improvements to the existing models were subsequently made and a new predictive model was presented. A comprehensive database of the tensile coupon tests from the companion paper [1] and existing experimental programs were used to validate the predictions from the models.

Analysis of the results showed that for the flat faces of cold-rolled stainless steel sections, the predictive model from Rossi [5] is able to predict more accurate results, in terms of the mean value, than the predictive equation proposed by Cruise and Gardner [4] but, has higher scatter. The results for the corner regions show that for stainless steel, the Cruise and Gardner [4] model offers more accurate predictions of the test data with lower scatter. Also, Rossi [5]

and the modified AISI model [13] predictions for the corner strength enhancements of carbon steel sections are in good agreement, with the former showing a lower scatter of 0.09. It was highlighted that while the Rossi [5] predictive model may be applied to any structural section of non-linear material, Cruise and Gardner's [4] model was developed solely for austenitic stainless steel structural sections. Also, Rossi's [5] predictive equation was considered too lengthy to implement in practical design calculations. In order to overcome the shortcomings of these models, a power law material model, with new strain measures, was proposed to predict the strength enhancement in cold-formed structural sections. Statistical analyses were carried out to ensure that the current level of reliability of the European design standards is maintained when the new predictive model is incorporated in design. The new proposed model provides good predictions of the test data, is simple to use in structural calculations and is applicable to any metallic structural sections.

Acknowledgements

The authors are grateful to the Outokumpu Research Foundation, the Steel Construction Institute and the University of Liège for their financial and technical contributions to the project.

References

[1] Afshan S, Rossi B, Gardner L. Strength enhancements in cold-formed structural sections – Part I: Material testing. Journal of Constructional Steel Research, 2013;83:177-188.

[2] EN 1993-1-4. Eurocode 3: Design of steel structures - Part 1-4: General rules - Supplementary rules for stainless steels. Brussels: European Committee for Standardization (CEN); 2006.

[3] EN 1993-1-1. Eurocode 3: Design of steel structures - Part 1-1: General rules and rules for buildings. Brussels: European Committee for standardization (CEN); 2005.

[4] Cruise RB, Gardner L. Strength enhancements induced during cold forming of stainless steel sections. Journal of Constructional Steel Research, 2008;64(11):1310-6.

[5] Rossi B. Mechanical properties, residual stresses and structural behavior of thin-walled stainless steel profiles. PhD Thesis. Belgium: University of Liège; 2008.

[6] Rossi B, Boman R, Degée H. Effects of the roll forming process on the mechanical properties of thin-walled sections made of non linear metallic materials. Sixth International Conference on Thin Walled Structures. Timisoara, Romania. 2011. p. 633-40.

[7] Quach W, Teng J, Chung K. Residual stresses in press-braked stainless steel sections, II: Press-braking operations. Journal of Constructional Steel Research, 2009;65(8):1816-26.

[8] Karren K. Corner properties of cold-formed steel shapes. Journal of the Structural Division, ASCE, 1967;93(1):401-32.

[9] Coetzee J, Van den Berg G, Van der Merwe P. The effect of work hardening and residual stresses due to cold-work of forming on the strength of cold-formed stainless steel lipped channel section. Tenth Intenational Speciality Conference on Cold-Formed Steel Structures. St. Louis, Missouri, USA, 1990. p. 143-62.

[10] Van den Berg G, Van der Merwe P. Prediction of corner mechanical properties for stainless steels due to cold forming. Eleventh International Speciality Conference on Cold-Formed Steel Structures. St. Louise, Missouri, USA, 1992. p. 571-86.

[11] Gardner L, Nethercot D. Experiments on stainless steel hollow sections—Part 1: Material and cross-sectional behaviour. Journal of Constructional Steel Research, 2004;60(9):1291-318.

[12] Ashraf M, Gardner L, Nethercot D. Strength enhancement of the corner regions of stainless steel cross-sections. Journal of Constructional Steel Research, 2005;61(1):37-52.

[13] Gardner L, Saari N, Wang F. Comparative experimental study of hot-rolled and cold-formed rectangular hollow sections. Thin-walled structures, 2010;48(7):495-507.

[14] Specification for the design of cold-formed steel structural members. American Iron and Steel Institute (AISI); 1996.

[15] Abdella K. Inversion of a full-range stress–strain relation for stainless steel alloys. International Journal of Non-Linear Mechanics, 2006;41(3):456-63.

[16] Guo YJ, Zhu AZ, Pi YL, Tin-Loi F. Experimental study on compressive strengths of thick-walled cold-formed sections. Journal of Constructional Steel Research, 2007;63(5):718-23.

[17] Niemi E, Rinnevalli J. Buckling tests on cold-formed square hollow sections of steel Fe 510. Journal of Constructional Steel Research, 1990;16(3):221-30.

[18] Zhu Y, Wilkinson T. Compression capacity of hollow flange channel stub columns. Research report R875. Sydney. 2007.

[19] Ala-Outinen T. Stainless steel in fire (SSIF). Work package 3: Members with Class 4 cross-sections in fire, ECSC project. Contract no. RFS-CR-04048. The Steel Construction Institute, UK. 2007.

[20] Cruise RB. The influence of production routes on the behaviour of stainless steel structural members. PhD Thesis. UK: Imperial College London; 2007.

[21] Gardner L. A new approach to structural stainless steel design. PhD Thesis. UK: Imperial College London; 2002.

[22] Gardner L, Talja A, Baddoo N. Structural design of high-strength austenitic stainless steel. Thin-walled structures, 2006;44(5):517-28.

[23] Hyttinen V. Design of cold-formed stainless steel SHS beam-columns. Report 41. Laboratory of Structural Engineering. Finland. University of Oulu. 1994.

[24] Rasmussen K, Hancock G. Design of cold-formed stainless steel tubular members. I: Columns. Journal of structural engineering, 1993;119(8):2349-67.

[25] Talja A, Salmi P. Design of stainless steel RHS beams, columns and beam-columns. Research note 1619. Finland. VTT building technology1995.

[26] Afshan S, Gardner L. Experimental study of cold-formed ferritic stainless steel hollow sections. Journal of Structural Engineering (ASCE), In press.

[27] Theofanous M, Gardner L. Experimental and numerical studies of lean duplex stainless steel beams. Journal of Constructional Steel Research, 2010;66(6):816-25.

[28] Lecce M, Rasmussen K. Experimental investigation of the distortional buckling of cold-formed stainless steel sections. Research Report R844, 2005.

[29] Ashraf M, Gardner L, Nethercot DA. Finite element modelling of structural stainless steel cross-sections. Thin-walled structures, 2006;44(10):1048-62.

[30] Rasmussen KJR. Full-range stress–strain curves for stainless steel alloys. Journal of Constructional Steel Research, 2003;59(1):47-61.

[31] EN 10088-1. Stainless steels - Part 1: List of stainless steels. Brussels: European Committee for Standardization (CEN); 2005.

[32] EN 1999-1-1. Eurocode 9: Design of aluminium structures - Part 1-1: General structural rules. Brussels: European Committee for standardization (CEN); 2007.

[33] Moen CD, Igusa T, Schafer B. Prediction of residual stresses and strains in cold-formed steel members. Thin-walled structures, 2008;46(11):1274-89.

[34] AS/NZS 4673. Cold-formed stainless steel structures. Sydney: Standards Australia; 2001.

[35] SEI/ASCE 8-02. Specification for the design of cold-formed stainless steel structural members. Reston: American Society of Civil Engineers (ASCE); 2002.

[36] Tests on stainless steel materials. Report no. SCI-RT-251. Steel Construction Institute. London1991.

[37] EN 1990. Eurocode - Basis of structural design. Brussels: European Committee for Standardization (CEN); 2002.

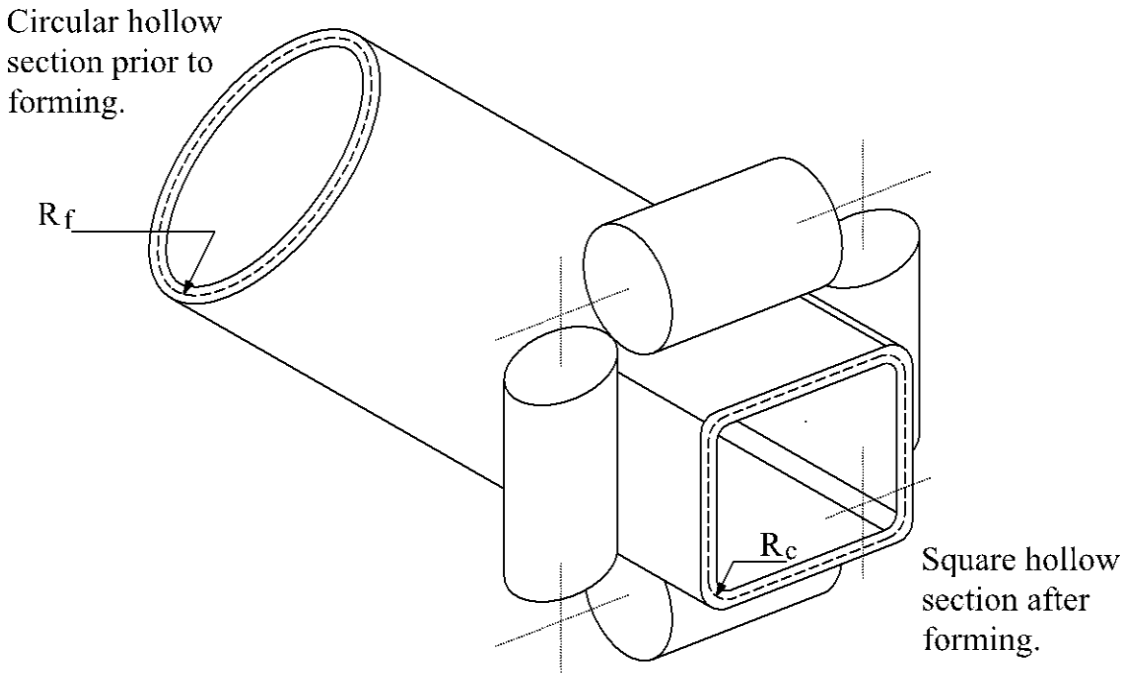

Fig. 1. Cold-rolling fabrication of tubular box sections.

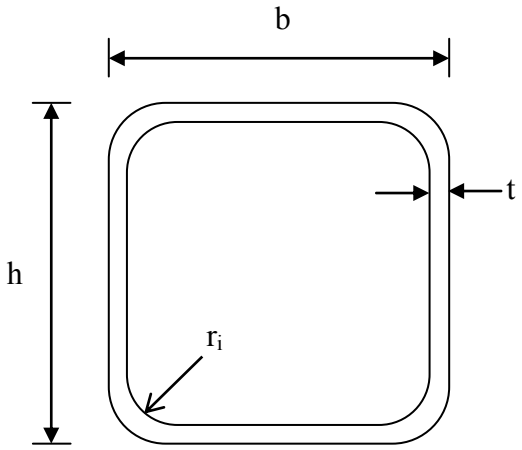

Figure 2. Definition of symbols for SHS and RHS.

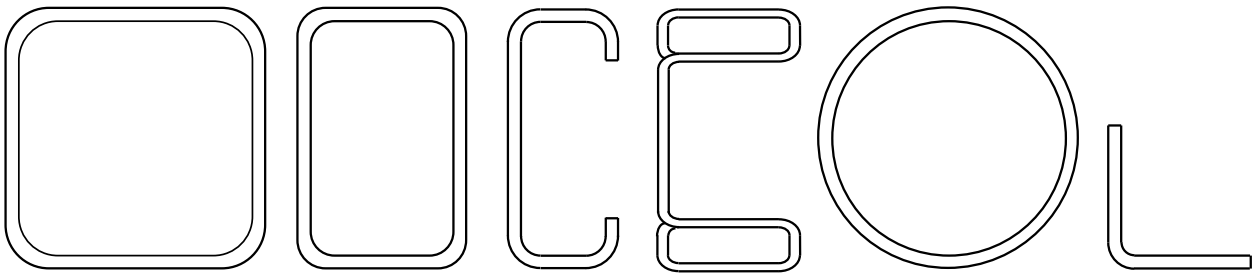

Figure 3. Variety of cold-formed cross-sections considered in this study.

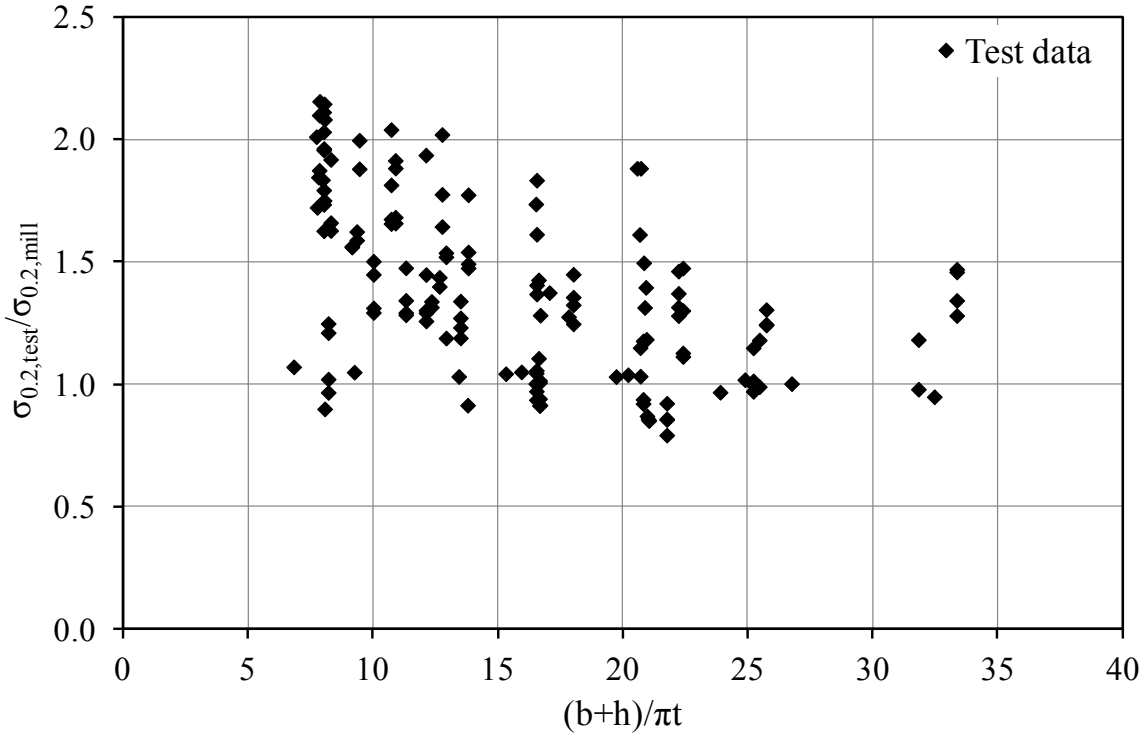

Figure 4. Normalised measured 0.2% proof stress for the flat faces of cold-rolled sections.

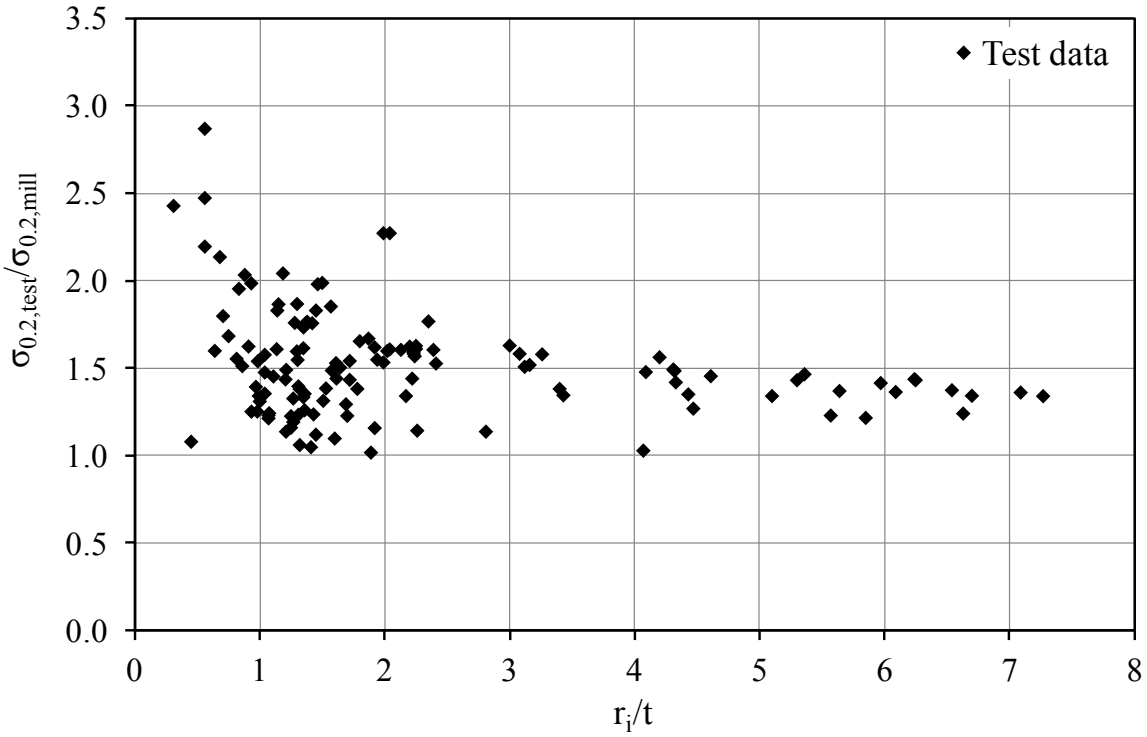

Fig. 5. Normalised measured 0.2% proof stress for the corner regions of cold-formed sections.

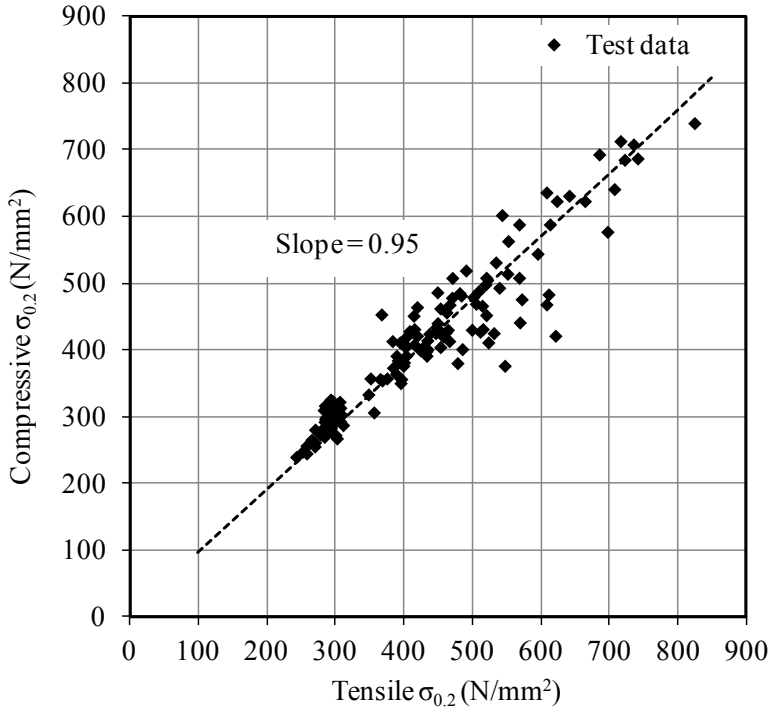

Figure 6. Relationship between the tensile and compressive 0.2% proof stress.

Table 1. Summary of database for coupon tests on flat material in cold-rolled sections.

Reference	Material	Section type	No. of tests
[1]	CS (S355)	SHS/RHS	12
[13]	CS (S235)	SHS,RHS	5
[16]	CS (S235)	SHS, RHS	6
[17]	CS (S355)	SHS	1
[18]	CS[(1)]	HFCS	19
[1]	SS (1.4301)	SHS/RHS	9
[1]	SS (1.4571)	SHS	6
[1]	SS (1.4404)	SHS/RHS	6
[19]	SS (1.4301)	SHS	4
[20]	SS (1.4301)	SHS,RHS	7
[21]	SS (1.4301)	SHS,RHS	54
[22]	SS (1.4318)	SHS,RHS	16
[23]	SS (1.4301)	SHS	8
[24]	SS (1.4306)	SHS	1
[25]	SS (1.4301)	SHS	10
[1]	SS (1.4003)	SHS/RHS	6
[26]	SS (1.4003)	SHS,RHS	12
[23]	SS (1.4003)	SHS	4
[1]	SS (1.4509)	SHS	9
[23]	SS (1.4512)	SHS	4
[1]	SS (1.4462)	CHS	2
[27]	SS (1.4162)	SHS,RHS	16
[1]	SS (1.4162)	SHS	3

Note: [(1)] Material grade was not reported.

Table 2. Summary of database for coupon tests on corner material.

Reference	Material	Section type	No. of tests
[1]	CS (S355)	SHS/RHS	8
[13]	CS (S235)	SHS/RHS	5
[16]	CS (S235)	SHS/RHS	6
[17]	CS (S355)	SHS	1
[18]	CS[(1)]	HFCS	12
[1]	SS (1.4301)	SHS/RHS	6
[1]	SS (1.4571)	SHS	4
[1]	SS (1.4404)	SHS/RHS	4
[9]	SS (1.4301)	LCS	4
[9]	SS (1.4401)	LCS	4
[20]	SS (1.4301)	SHS/RHS	27
[20]	SS (1.4301)	Angle	8
[21]	SS (1.4301)	SHS/RHS	5
[22]	SS (1.4318)	SHS/RHS	2
[28]	SS (1.4301)	LCS	2
[24]	SS (1.4306)	SHS	1
[10]	SS (1.4301)	Angle	9
[1]	SS (1.4003)	SHS/RHS	4
[26]	SS (1.4003)	SHS/RHS	3
[9]	SS (1.4003)	LCS	4
[28]	SS (1.4016)	LCS	2
[28]	SS (1.4003)	LCS	2
[10]	SS (1.4512)	Angle	10
[10]	SS (1.4016)	Angle	9
[10]	SS (1.4003)	Angle	10
[1]	SS (1.4162)	SHS	2
[27]	SS (1.4162)	SHS/RHS	4

Note: [(1)] Material grade was not reported.

Table 3. Comparison of the predictive models and test data for the 0.2% proof strength of the flat faces of cold-rolled sections ($\sigma_{0.2,f,pred}/\sigma_{0.2,test}$)

Predictive Model		Cruise and Gardner [4]	Rossi [5]
All	Mean	1.10	0.97
	COV	0.21	0.20
Carbon steel	Mean	(1.25)	0.99
	COV	(0.20)	0.18
Stainless steel	Mean	1.06	0.97
	COV	0.20	0.21

Table 4. Comparison of the predictive models and test data for the 0.2% proof strength of the corner regions of cold-formed sections ($\sigma_{0.2,c,pred}/\sigma_{0.2,test}$)

Predictive Model		Cruise and Gardner [4] / Gardner at al. [13]	Rossi [5]
All	Mean	0.97	1.06
	COV	0.11	0.14
Carbon steel	Mean	0.97	0.98
	COV	0.11	0.09
Stainless steel	Mean	0.97	1.08
	COV	0.12	0.14

Table 5. Comparison of the proposed predictive models and test data for the 0.2% proof strength of flat faces of cold-rolled sections ($\sigma_{0.2,f,pred}/\sigma_{0.2,test}$)

Predictive Model		Linear model	Power model
All	Mean	0.89	1.01
	COV	0.21	0.20
Carbon steel	Mean	0.96	1.00
	COV	0.17	0.19
Stainless steel	Mean	0.87	1.01
	COV	0.22	0.20

Table 6. Comparison of the proposed predictive models and test data for the 0.2% proof strength of corner regions of cold-formed sections ($\sigma_{0.2,c,pred}/\sigma_{0.2,test}$)

Predictive Model		Linear model	Power model
All	Mean	0.92	0.96
	COV	0.14	0.14
Carbon steel	Mean	0.93	0.92
	COV	0.07	0.08
Stainless steel	Mean	0.92	0.97
	COV	0.16	0.15